Available online at www.sciencedirect.com
SCIENCE DIRECT®

Journal of the European Ceramic Society 23 (2003) 2125–2133
www.elsevier.com/locate/jeurceramsoc

Processing and characterisation of a fine nickel oxide/zirconia/composite prepared by polymeric complex solution synthesis

P. Durán*, J. Tartaj, F. Capel, C. Moure

Instituto de Ceramica y Vidrio, CSIC, Electroceramics Department, 28500 Arganda del Rey, Madrid, Spain

Received 29 June 2002; received in revised form 9 December 2002; accepted 15 December 2002

Abstract

A homogeneous dispersion of nickel in a YSZ ceramic matrix by the polymeric organic complex solution method was achieved. A YSZ powder was added to the polymeric gel containing Ni^{2+} cations leading to an organic resin in which the YSZ particles were embedded. By further heat treatment a composite of ultrafine nickel oxide dispersed in the YSZ matrix was attained. After sintering and reducing treatment of nanocrystalline NiO/YSZ composite, the microstructure of the Ni/YSZ cermet showed a uniform distribution of the porous metallic Ni particles of about 1–2 μm surrounded by a microporous space. The electrical properties of NiO/YSZ (55/45 wt.%) composites were studied using impedance spectroscopy in the temperature range from 100 to about 700 °C. Variations in activation energy were in agreement to the NiO electrical behaviour with increasing temperatures for polymer complex solution NiO/YSZ prepared composite, which indicates a uniform and fine-grained microstructure, in which the YSZ–YSZ and/or the NiO–NiO particle contacts were predominant.

Keywords: Chemical synthesis; Fuel cells; NiO; ZrO_2; Composites; Anode

1. Introduction

Due to the high catalytic activity of Ni for fuel oxidation, a nickel oxide–yttria-stabilised zirconia (NiO/YSZ) composite is the most commonly anode material used for solid oxide fuel cells, SOFCs. The role of the metallic nickel is to make the anode, an electrical conductor, as high as possible at the operating conditions of the SOFC device. Although the electrical behaviour of a NiO/YSZ composite can be explained by percolation theory but it is not less important the contribution of the microstructure for a satisfactory behaviour of the Ni/YSZ anode material. On the other hand, since such a microstructural contribution depends on reciprocal size of the YSZ and Ni grains,[1] the higher efficient Ni/YSZ anode material will be that having fine Ni particles uniformly distributed in the YSZ matrix. In that way, a satisfactory Ni/YSZ anode material behaviour was reported for both, small Ni grains surrounding larger YSZ grains or NiO particles surrounded by YSZ thin films.[1–4] Therefore, it seems clear that the morphology of the NiO and YSZ particles play an important role in the conductivity of the Ni/YSZ anode material.

Currently, the method used for anode manufacturing is mechanical mixing of NiO and YSZ powders, but due to the large difference in powder density a separation of NiO and YSZ particles can occur during handling a slurry of NiO and YSZ powders. As a final consequence the Ni particles will be non-uniformly distributed in the YSZ matrix and some degradation problems can be present during service.[5] Therefore, the development of a process as simple as possible leading to produce NiO/YSZ powder having fine Ni particles uniformly distributed in the anode material, is an objective intensively investigated. Several routes such as coprecipitation, freeze-drying and solid-state synthesis have been widely used to prepare small particle sized powders,[6,7] but the preparation of complex metal oxides by the combustion synthesis has recently become an important area of research because of promising results of this technique

* Corresponding author. Tel.: +34-91-871-1800; fax: +34-91-870-0550.
E-mail address: pduran@icv.csic.es (P. Durán).

0955-2219/03/$ - see front matter © 2003 Elsevier Science Ltd. All rights reserved.
doi:10.1016/S0955-2219(03)00028-1

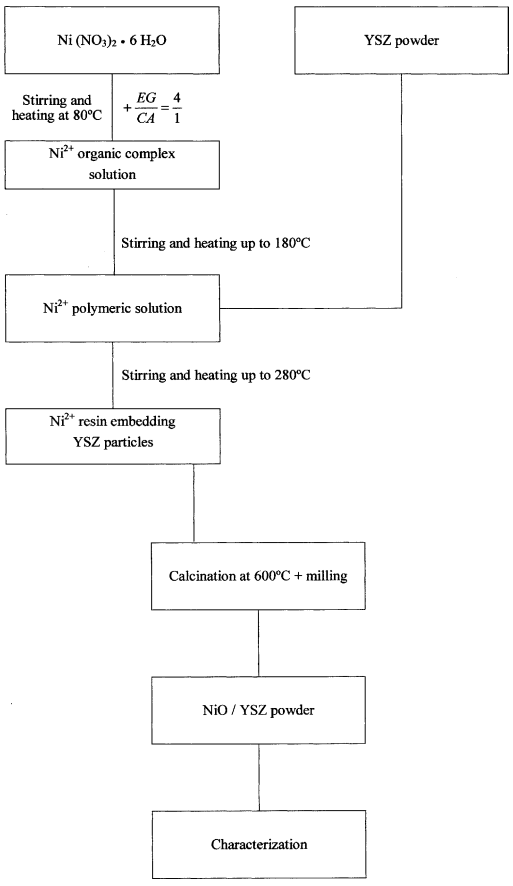

Fig. 1. Flow chart for preparing NiO–YSZ composite powders.

compared to the conventional method.[3] Currently, powders with good sinterability have been obtained using mixtures with carboxylate, urea and/or glycine,[8,9] with the additional advantage of obtaining the complex oxide powders directly from the precursor solution. Therefore, the combustion synthesis could be, in principle, a good method leading to prepare the composite powder of Ni/YSZ with uniform distribution of fine Ni particles, if some problems like the thermal explosion with no control of the synthesis temperature, are avoided.

In order to overcome the mentioned difficulties, in the present work a modified Pechini method was used to prepare the NiO/YSZ composite, in which ultrafine NiO particles uniformly distributed in the composite is the main characteristic of this preparation method.[10,11] A YSZ powder suspension in an aqueous solution of citric acid/ethyleneglycol/metal salt was used. The distribution of NiO particles in the as prepared NiO/YSZ powder was evaluated on the sintered samples. Microstructure and electrical properties have also been studied and compared with samples prepared by mechanical mixing.

2. Experimental procedure

Samples of the composition NiO/YSZ = 55/45 wt.% were prepared by a modified Pechini method. Such a

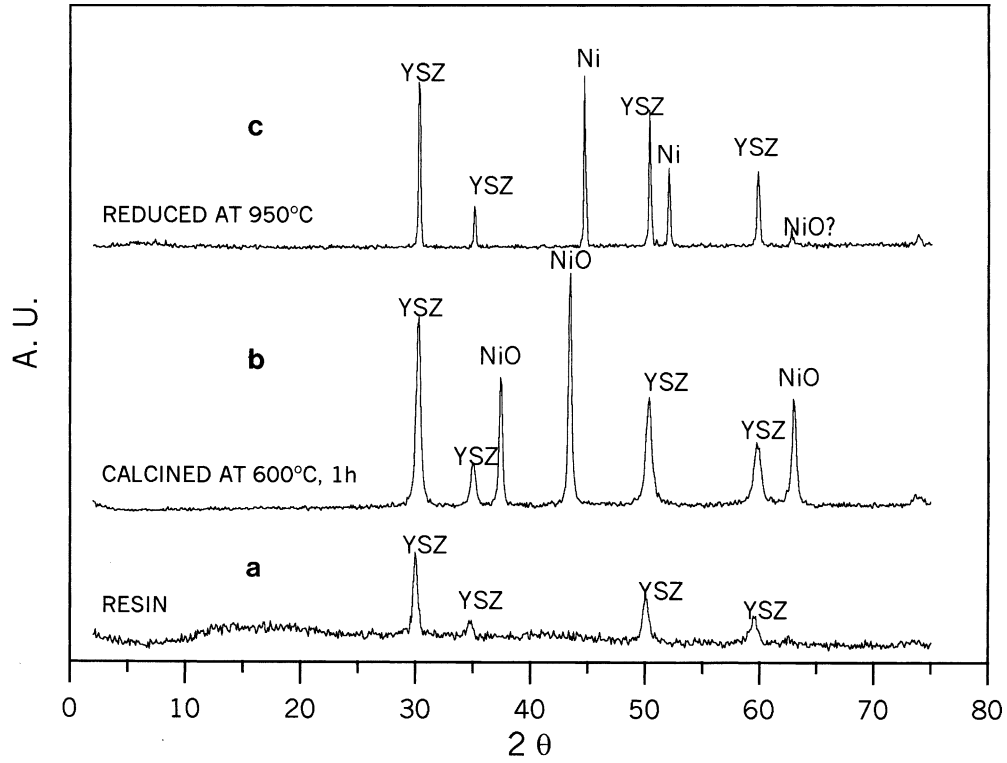

Fig. 2. XRD patterns of as-synthesized NiO–YSZ powders made by the complex polymer solution, (a) resin, (b) calcined at the indicated temperature, and (c) after reduction in 90 N_2–10 H_2 at the indicated temperature.

composition was chosen because it is located above the threshold of percolation.[1] Firstly, an aqueous solution of $Ni(NO_3)_2{\cdot}6H_2O$ was mixed by stirring with the required amount of citric acid (CA) and ethyleneglycol (EG), molar ratio CA/EG = 1/4, and heated at 60 °C for 2 h. The as-obtained transparent solution was successively heated at 80 and 180 °C for 2 h, leading to an almost transparent viscous polymeric solution. At this point the YSZ powder was added by vigorous stirring. After heating at 280 °C for 2 h a black resin embedding the YSZ particles was obtained hereinafter labelled as P–Ni/YSZ sample. After grinding, the resin was calcined at 600 °C for 1 h and attrition milled for 1 h in methanol with zirconia ball media. The identification of phases was made using a diffractometer Siemens (model D-5000, Erlangen, Germany), with CuK_α radiation and Ni filter, and the BET surface area of the calcined powder was measured using a Quantachrome Accusorb instrument. The particle size and morphology of the as prepared powders were determined by transmission electron microscopy using a Hitachi Instrument. Fig. 1 shows the flow sheet for the NiO/YSZ composite powder preparation.

After milling, the powder was dried and uniaxially pressed into pellets at 100 MPa, then sintered in air at 1500 °C for 1 h. To investigate the influence of NiO morphology contribution on cermet behaviour, a cermet was made by using the conventional mixing oxide method with Tosoh YSZ and NiO powders, hereinafter labelled as O–Ni/YSZ sample with the same NiO content as that prepared by the Modified Pechini method (55 wt.% NiO), and the shrinkage characteristics were observed using a dilatometer Netzsch (model 407/E, Selb-Bayern Germany). The sample temperature was raised to 1500 °C at a constant heating rate (CHR) of 3 °C/min. After sintering, the samples were reduced using a N_2 90%/H_2 10% atmosphere at 1000 °C for 4 h.

The microstructure of the sintered samples was examined in a Zeiss Microscope (model DSM 950, Oberkochem, Germany), on the polished and thermally etched surface, and the grain size of both NiO and YSZ phases was measured by the interception method. Impedance was measured from room temperature up to 700 °C in air using a LF Impedance Analyser (Model 4192A, Hewlett-Packard).

3. Experimental results

Fig. 2 shows typical X-ray diffraction (XRD) patterns of NiO/YSZ resin, calcined and reduced composite powder synthesised by the polymer complex solution method. As it can be observed, the XRD pattern of the powder resin was a composite of Ni^{2+}-containing amorphous organic matter, because no new peaks appeared except for those of the YSZ crystalline phase. After calcining, the as synthesised powder was a composite consisting of NiO and YSZ crystalline phases and after reduction Ni metal, NiO traces and YSZ phases were present. Fig. 3 shows SEM microphotograph of the same composite powder. The particles of YSZ powder was embedded in the resin containing Ni^{2+} cation complexes, as it is shown in Fig. 3A, and it had a friable and porous structure after calcining at 600 °C for 1 h (Fig. 3B). The calcined P–Ni/YSZ composite was a very sinterable powder with a specific surface area of 16 m^2/g, and an average agglomerated particle size ($D = 50\%$) of 0.9 μm. The calculated equivalent particle diameter, taking into account the BET specific surface and the theoretical

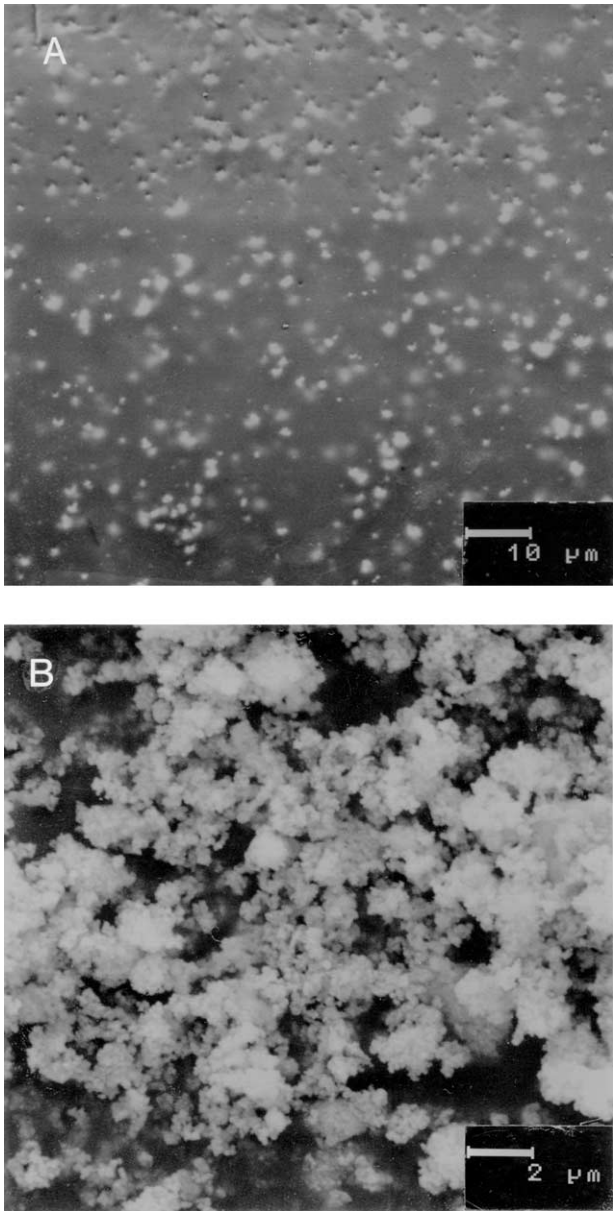

Fig. 3. SEM photographs of as-synthesized NiO–YSZ powder, (A) resin showing the YSZ embedded particles, and (B) P–Ni/YSZ calcined powder.

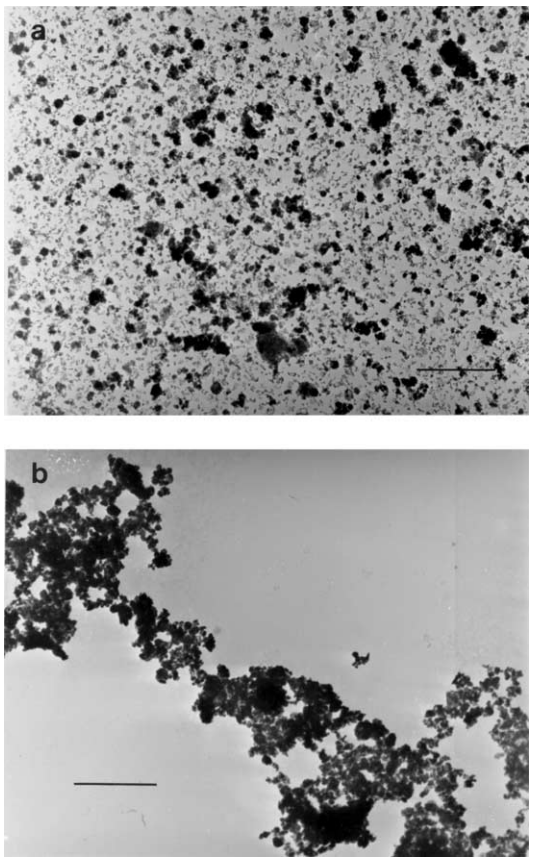

Fig. 4. TEM photographs of the two NiO–YSZ composite powders, (a) P–Ni/YSZ sample and (b) O–Ni/YSZ sample, (bar = 1 μm).

density of the calcined P–Ni/YSZ composite, (6.37 g/cm^3) was of 0.059 μm, which indicates a certain agglomeration level after milling, comparing with that measured by XRLB, which was of 0.022 μm. The morphology of the P–Ni/YSZ nanosized powders as well as that of the O–Ni/YSZ powders is shown in Fig. 4. A white phase, (NiO), and a black one, (YSZ) with particles or agglomerates sizes in the range of 0.015 and 0.3 μm, respectively, can be observed in the TEM micrographs.

After compaction, the microstructure of the green compacts was quite different in both cases, the P–Ni/YSZ prepared sample showed a very uniform distribution of the NiO particles between the YSZ particles while higher dispersion was present in the case of mechanically mixed oxide prepared samples. Fig. 5 shows the shrinkage behaviour of the two kind of NiO/YSZ fired samples up to 1500 °C. As it can be observed, the behaviour is quite similar in both cases. The sintering shrinkage of both samples began at a relatively low temperature (900 °C), but a lower end point temperature was achieved for the P–Ni/YSZ prepared sample, and a slightly higher density was attained, 99 against 98.5% D_{th}. Shrinkage of 22 against 20%, respectively, at the end of the firing process took place in the samples. As a summary it may be concluded that although the shrinkage characteristics of both composites are very similar, but the shrinkage difference among them, being the same used YSZ in both cases, can be due to the sintering characteristics of the NiO powder.

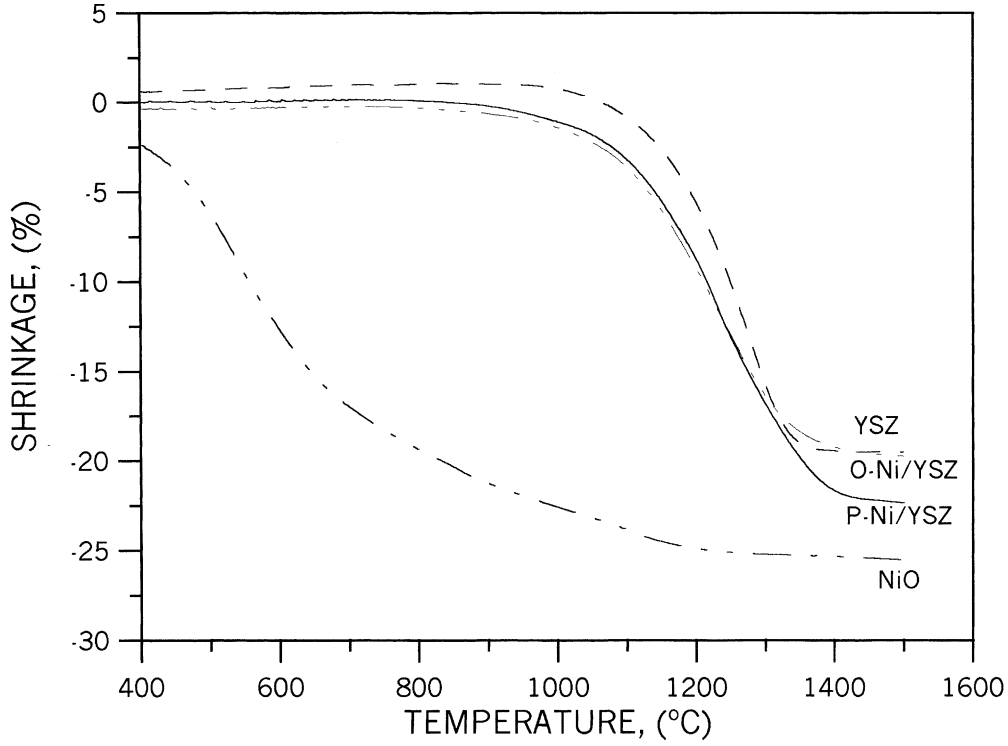

Fig. 5. Shrinkage behaviour of P–Ni/YSZ, O–Ni/YSZ, YSZ and NiO green compacts vs. temperature.

Fig. 6 shows the backscattered electron image of the sintered samples, along with the characteristic energy dispersive X-ray (EDX) spectra of the individual present phases. EDX analysis revealed that the greenish grains are NiO, (labelled "a") and brighter-looking grains are YSZ, (labelled "b"). This phase contained a very small amount of NiO, which is in agreement with the low NiO solid solution in YSZ. A quantitative analysis of the YSZ grains gave an average percentage of 78.67% ZrO_2, 17.15% $YO_{1.5}$ and 4.19% NiO, which is closed to the data reported for YSZ–NiO system.[1] A more detailed distribution of the NiO and YSZ phases is given in Fig. 7, which is an SEM micrograph of the non-etched polished surfaces of the sintered samples. This figure shows that the microstructure of the P–Ni/YSZ composite was dense and fine-grained, with a very homogeneous distribution of the two NiO and YSZ phases.

Fig. 8a–f shows the microstructure of NiO/YSZ composites sintered at 1500 °C without holding. For comparison, the microstructure of YSZ and NiO sintered at the same temperature are also shown. Although the contrast between nickel and YSZ is very low because of the small difference in average atomic weight, by using back-scattered electrons it was possible to distinguish with relative clarity between the darkish NiO grains and the brighter YSZ grains. Furthermore, the edge of the NiO grains is also sharper and striped than that of the

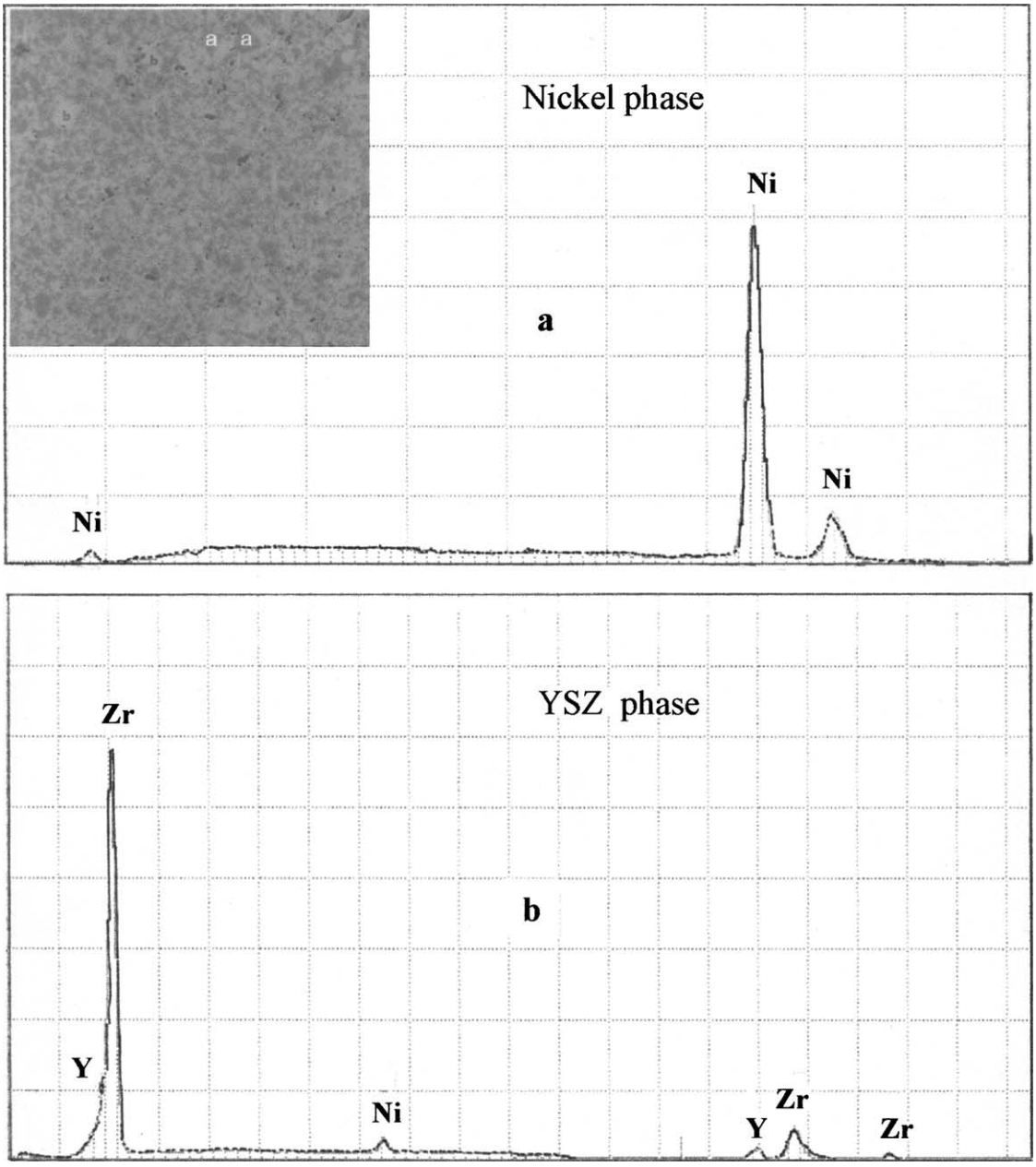

Fig. 6. SEM backscattered electron image of the P–Ni/YSZ sintered sample along with its EDX spectra.

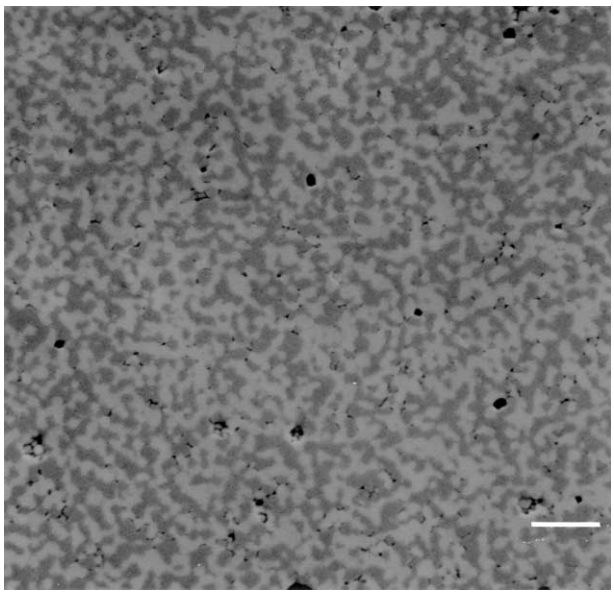

Fig. 7. SEM backscattered electron photograph of the polished and unetched surface of sintered P–Ni/YSZ sample (bar = 10 μm).

YSZ. Other differential feature to distinguish the NiO grains is the appearance of an additional porosity on its surface as consequence, probably, of oxygen lost during sintering. It must be mentioned that the YSZ powders, which had an initial spherical morphology (diameter ~30–50 μm) were broken during the ball-milling process to a finer powder (~0.3 μm). As can be observed, the average grain size of YSZ was between 3 and 4 μm with a size distribution quite homogeneous (Fig. 8a). It has been reported that the presence of NiO grains, intergranularly located, retards the grain growth of YSZ grains[1] and, thus, the YSZ grain size increased only up to about 2 μm in the P–Ni/YSZ sample and less than 2 μm in the O–Ni/YSZ one (Fig. 8b and c). It should be mentioned that the grain size of the NiO particles in the composites was slightly larger and more uniformly distributed in the P–Ni/YSZ sample (~2.5–3 μm) comparatively to that of the O–Ni/YSZ samples that was almost the same magnitude of the YSZ grains, (~1–2μm). The grain size of the sintered NiO alone was about 10 μm (Fig. 8d). After reduction, the microstructure of the P–Ni/YSZ showed a uniform distribution of porous/spherical Ni particles trapped into the YSZ ceramic matrix (Fig. 8e). The Ni particles were about 2 μm in size, which indicates no grain growth during the reduction process.

Given that the anode may undergo many thermal cycles at the operating SOFC conditions, it should be desirable that the thermal expansion coefficient of this material match that of the electrolyte. If this is not so, then a separation between them can take place with the consequent failure of the device. Therefore, the thermal expansion of the NiO/YSZ anode, YSZ electrolyte and NiO were studied in the temperature range of 25 to 1000 °C. Fig. 9 shows the thermal expansions of the ceramic materials in air at a heating rate of 5 °C/min. As it can be observed, the slopes of the thermal expansion vs temperature curves increase with increasing NiO content, i.e., NiO > NiO/YSZ ⩾ YSZ. The calculated thermal expansion coefficients were $14.5 \pm 0.5 \times 10^{-6}$, $12.7 \pm 0.5 \times 10^{-6}$ and $11 \pm 0.5 \times 10^{-6}$ K^{-1} for NiO, NiO/YSZ and YSZ respectively. These values are somewhat higher than those reported in the literature.[12]

Fig. 10 shows the impedance spectra of NiO/YSZ composites measured at 250 °C. As it is well known,[13] we also assume that the higher frequency arc represents the resistance of the bulk and the medium frequency arc is representing the grain boundary resistance. At the mentioned temperature, two overlapping semicircles at high and medium frequencies were present. With increasing temperature a third semicircle, rather a tail, started to appear at low frequency. From the electrical data obtained before reduction and taking into account the Arrhenius equation, several temperature intervals with different activation energies were detected. In the P–Ni/YSZ samples an activation energy of 0.92 eV was calculated between 125 and 350 °C, and energies of 0.38 and 0.20 eV were calculated between 350 and 450 °C and between 450 and 650 °C respectively. Fig. 11 shows the Arrhenius plot for the P–Ni/YSZ composite, and Table 1 summarises electrical data at 450 °C, for different NiO/YSZ composites.

4. Discussion

NiO/YSZ submicronised composite powders were successfully prepared by the polymer complex solution method using YSZ, $Ni(NO_3)_2 \cdot 6H_2O$, ethyleneglycol and citric acid as the starting materials. According to our results (Fig. 3a), an organic Ni^{2+}-containing ceramic matrix embedding homogeneously distributed YSZ particles was obtained. After calcining a NiO/YSZ nanocomposite powder in which the NiO nanoparticles surrounded the larger YSZ ones was obtained (see Fig. 4). Although a slight difference in the shrinkage behaviour for the two substrates was found, the sinterability of the NiO powder also has a significant influence on the sintering behaviour of the NiO/YSZ composites. Such an influence led to a microstructure in which the higher contraction of the NiO particles allowed the normal sintering process of the YSZ ceramic phase with the trapped NiO particles. In this case, it seems to be that the NiO particles did not form a continuous phase and limited, after reduction, the nickel to nickel particle contacts. As is shown in the Fig. 8e, the spherical Ni particles were surrounded by the YSZ ceramic powder.

It is now well known that the electrode performance of a Ni–YSZ cermet for SOFC's is very dependent on the microstructure and the distribution of Ni in YSZ

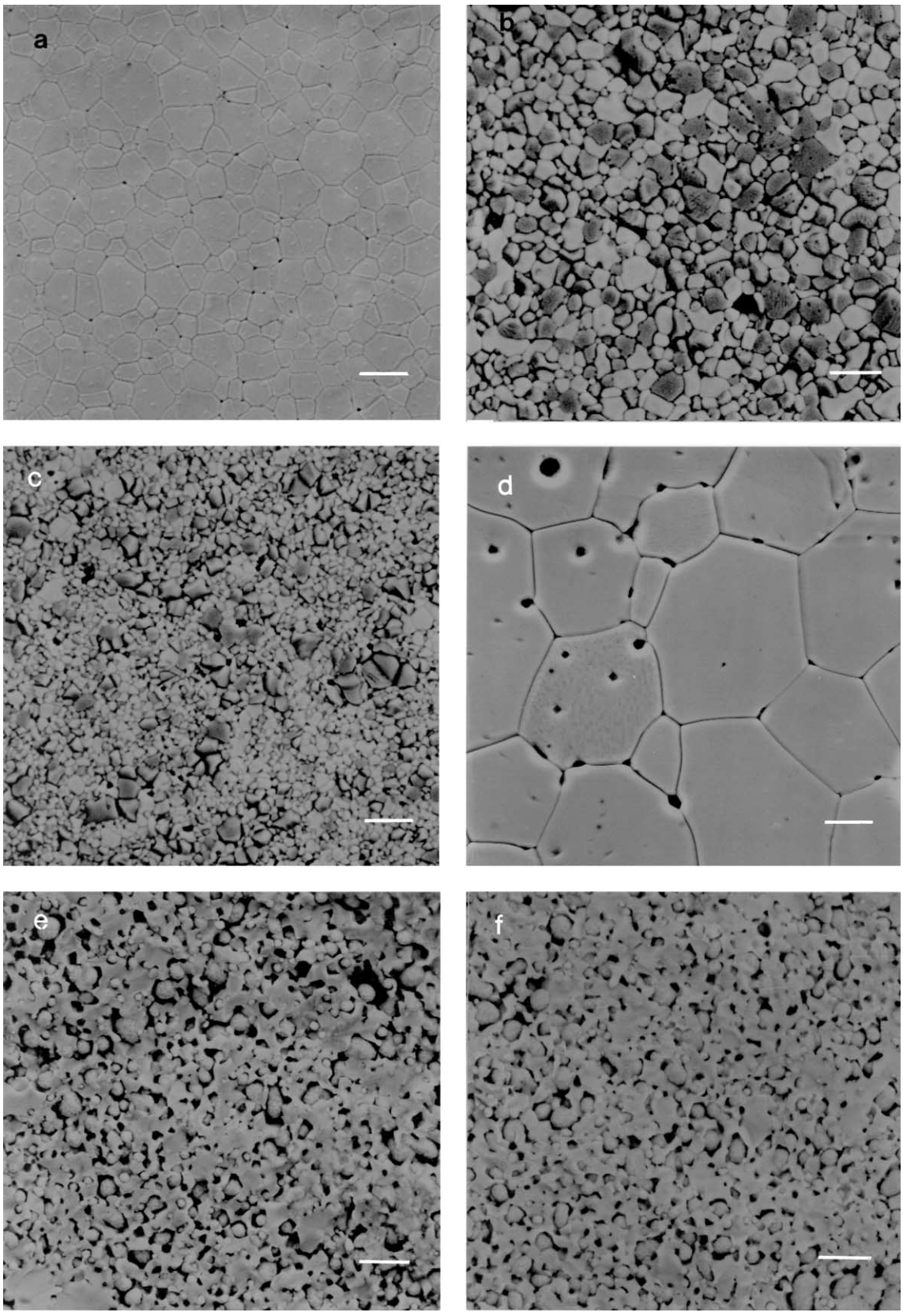

Fig. 8. SEM photographs of the microstructure, (a) YSZ, (b) P–Ni/YSZ, (c) O–Ni/YSZ, and (d) NiO, all of them sintered at 1500 °C: (e) and (f) are the P–Ni/YSZ and O–Ni/YSZ sintered samples after reduction in 90 N_2–10 H_2 (bar = 5 μm).

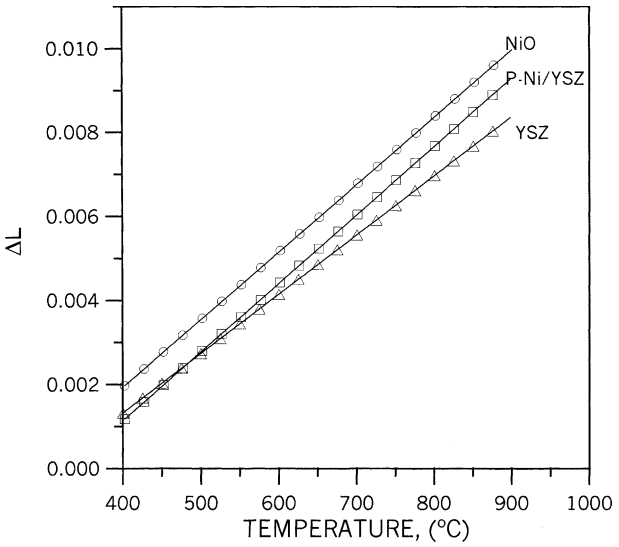

Fig. 9. Thermal expansion vs. temperature plot of NiO, YSZ, and P–Ni/YSZ samples.

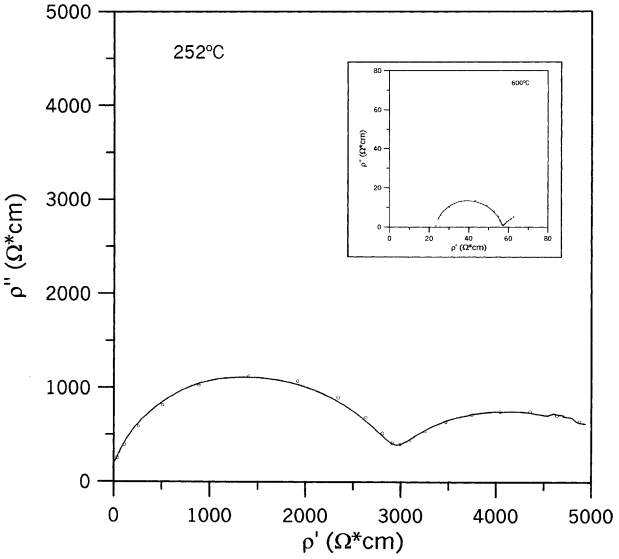

Fig. 10. Complex impedance spectrum of P–Ni/YSZ composite recorded at 252 °C in air. (Complex impedance spectrum recorded at 600 °C is shown in the insert.)

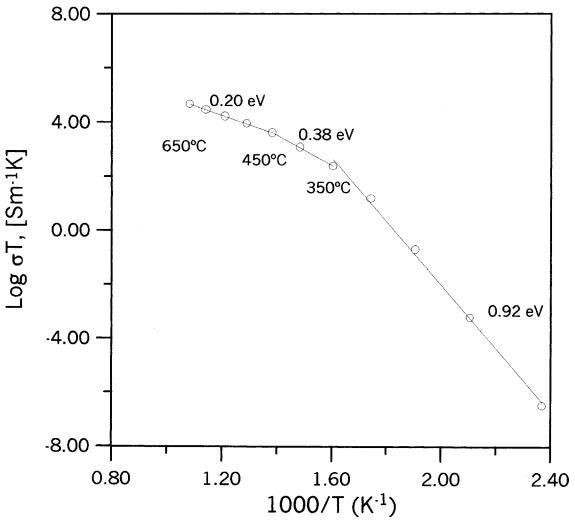

Fig. 11. Arrhenius plot for the total electrical conductivity of the P–Ni/YSZ sample.

Table 1

Samples	Vol.% NiO	σ, 450 °C, S cm^{-1}	E_a (eV)
P–Ni/YSZ	52	2×10^{-4}	0.92 (125–350 °C) 0.38 (350–450 °C) 0.20 (450–650 °C)
Ni–YSZ[14]	50	5×10^{-4}	0.78 (160–400 °C) 0.31 (500–600 °C)
Ni–YSZ[20]	27	2.9×10^{-5}	0.40 (350–500 °C)

phases.[14] In the present work an almost ideal distribution of the NiO particles was achieved, which is much better than the results obtained for other combustion methods[9,15,16] (see Fig. 8b). Such a microstructure can improve the area among gas, Ni and YSZ in the triple phase boundary, TPB, which is defined as the region encompassing the electron conductor (Ni), ion conductor (YSZ) and the gaseous reactants (H_2).[17] The electrode polarisation phenomena occurring during the SOFC service are strongly related to the length of such a region.

According to our results (see Fig. 10), it seems to be that for a NiO concentration of 52 vol.%, i.e. above the percolation threshold, the conduction in the NiO/YSZ composites would be due to the oxygen ions in YSZ and holes in NiO in the temperature range of 125–350 °C in air. The calculated activation energy (0.92 eV) is near to the average value of the individual activation energies, 1.01 and 0.88 eV for YSZ and NiO, respectively.[18,19] This means that the main charge carriers are electronic holes of NiO and the conduction mechanism is governed by the lower oxygen vacancy mobility in the lower temperature region. With increasing temperature the mobility of the oxygen vacancies becomes higher and that of the holes of NiO lower. Therefore, the main charge carriers above 300 °C are predominantly oxygen vacancies of YSZ, and the conduction mechanism is governed by the lower mobility of the holes of NiO. Consequently, the activation energy for the electrical conduction is much lower (see Fig. 11). When comparing the total electrical conductivity of different samples at a fixed temperature (450 °C) see (Table 1), it is noteworthy that this is lower for those samples with the more uniform microstructure and, with the smaller grain size. This means that the total electrical conductivity is determined by the grain boundary resistance, and the grain boundary density is much higher in the case of the polymer complex solution prepared samples. To confirm such a statement, our results were also compared with a mesoporous YSZ containing NiO nanoclusters[20] (see Table 1). There was a lower total conductivity

(2.9×10^{-5} S cm^{-1}), i.e., one order of magnitude lower than in our case, and although the NiO concentration (27 wt.%) was below the percolation threshold, the low total electrical conductivity was also attributed to an extremely high grain boundary density. A similar behaviour was also reported for NiO/YSZ compositions with NiO content above the percolation threshold,[14] in which although percolative behaviour was shown, a fast decreasing of the activation energy from 1.1 to 0.4 eV when passing from the low to the high temperature regions, was observed. Such an observation supported our contention for a transition between ionic to electronic dominance conduction mechanism with temperature.

5. Conclusions

A novel synthetic strategy by suspending powders of YSZ in a Ni^{2+} polymeric organic complex solution for the preparation of a NiO/YSZ (55/45 wt.%) composite was carried out. After calcining, a nanoscale nickel oxide uniformly dispersed throughout the YSZ ceramic powder was produced. Upon sintering the shrinkage behaviour of composite is affected by the sinterability of the NiO powder. The sintered NiO/YSZ composite showed an almost ideal microstructure in which fine NiO grains of about 2 μm were intergranularly distributed within the ceramic matrix. After reducing treatment porous Ni metal spherical particles were surrounded by a pore space and by the YSZ particles that can improve the TPB area between gas, Ni and YSZ. The mixed oxygen ion-electronic conduction is governed by the conduction behaviour of a probably non-stoichiometric NiO with increasing temperature. The relatively low total conductivity of the NiO/YSZ composite at the lower temperature range can be explained in terms of the high grain boundary density, which increased the grain boundary resistance. Activation energy in the high temperature range was quite lower than for conventional NiO/YSZ composites suggesting an improved NiO–NiO connectivity. The enhanced both microstructural and electrical properties of the as prepared NiO/YSZ composite indicate the suitability of the proposed preparation method for the manufacture of SOFC anodes.

Acknowledgements

The CICYT MAT2000-0815 Project supported this work.

References

1. Dees, D. W., Clark, T. D., Easler, T. E., Fee, D. C. and Mrazek, F. C., Conductivity of porous Ni/ZrO_2–Y_2O_3 cermets. *J. Electrochem. Soc.*, 1987, **134**, 2141–2146.
2. Tintinelli, A., Rizzo, C., Giunta, G. and Selvagi, A., Ni–YSZ porous cermets: microstructure and electrical conductivity. In *Proceedings of the 1st European SOFC Forum*, ed. U. Bossel and D. J. Kinzel. Gottingen, Germany, 1994, pp. 455–474.
3. Simwonis, D., Naounidis, A., Dias, F. J. and Linke Meropoucou, J., Material characterisation in support of the development of an anode substrate for solid oxide fuel cells. *J. Mater. Res.*, 1997, **12**, 1508–1518.
4. Itoh, H., Yamamoto, T., Mori, M., Horita, T., Sakai, N., Yokokawa, H. and Dokiya, M., Configurational and electrical behaviour of Ni–YSZ cermet with novel microstructure for solid oxide fuel cell anodes. *J. Electrochem. Soc.*, 1997, **144**, 641–646.
5. Jiang, S. P., Callus, P. J. and Badwal, S. P. S., Fabrication and performance of Ni/3 mol% Y_2O_3–ZrO_2 cermet anodes for solid oxide fuel cells. *Solid State Ionics*, 2000, **132**, 1–14.
6. Macek, J. and Marinsek, M., Coprecipitation process for preparation of nickel cermet anodes. In *Proceedings of the 2nd European SOFC Forum*, ed. B. Thorstensen and D. J. Kinzel. Gottingen, Germany, 1996, pp. 341–350.
7. Macek, J. and Marinsek, M., Thermal processing of Ni–YSZ. In *Proceedings of the 2nd European SOFC Forum*, ed. B. Thorstensen and D. J. Kinzel. Gottingen, Germany, 1996, pp. 351–360.
8. Kim, S. J., Jung, C. H. and Kim, Y. S., Synthesis of ultrafine Ni–YSZ powders by glycine nitrate process. In *Proceedings of the 2nd European SOFC Forum*, ed. B. Thorstensen and D. J. Kinzel. Gottingen, Germany, 1996, pp. 321–330.
9. Kim, S. J., Lee, W., Lee, W. J., Park, S. D., Song, J. S. and Lee, E. G., Preparation of nanocrystalline nickel oxide–yttria stabilised zirconia composite powder by the solution combustion with ignition of glycine fuel. *J. Mater. Res.*, 2001, **16**, 3621–3627.
10. Pechini, M. P. *Method of Preparing Lead and Alkaline Earth Titanates and Niobates and Casting Methods Using the Same to Form a Capacitor*. US Patent No 3.330.697, 11 July 1967.
11. Duran, P., Capel, F., Tartaj, J. and Moure, C., Sintering behaviour and electrical properties of nanosized doped–ZnO powders produced by metal–organic polymer processing. *J. Am. Ceram. Soc.*, 2000, **84**, 1661–1668.
12. Mori, M., Yamamoto, T., Itoh, H., Inaba, H. and Tagawa, H., Thermal expansion of nickel-zirconia anodes in solid oxide fuel cells during fabrication and operation. *J. Electrochem. Soc.*, 1998, **145**, 1374–1381.
13. McDonald, J. R., *Impedance Spectroscopy*. John Wiley & Sons, New York, 1987 pp 27.
14. Park, Y. M. and Choi, G. M., Microstruture and electrical properties of YSZ–NiO composites. *Solid State Ionics*, 1999, **120**, 265–274.
15. Aruna, S. T., Muthuraman, M. and Patil, K. C., Synthesis and properties of Ni–YSZ cermet: anode material for solid oxide fuel cells. *Solid State Ionics*, 1998, **111**, 45–51.
16. Minh, N. Q., Ceramic fuel cells. *J. Am. Ceram. Soc.*, 1993, **76**, 563–588.
17. Verweij, H., Nanocrystalline and nanoporous ceramics. *Adv. Mater.*, 1998, **10**, 1483–1486.
18. Park, Y. M. and Choi, G. M., Mixed ionic and electronic conduction in YSZ–NiO composite. *J. Electrochem. Soc.*, 1999, **146**, 883–889.
19. Majumdar, S., Claar, T. and Flandermeyer, B., Stress and failure behaviour of monolithic fuel cell tapes. *J. Am. Ceram. Soc.*, 1986, **69**, 628–633.
20. Mamak, M., Coombs, N. and Ozin, G. A., Electroactive mesoporous yttria stabilised zirconia containing platinum or nickel oxide nanoclusters: a new class of solid oxide fuel cell electrode materials. *Adv. Funct. Mater.*, 2001, **11**, 59–63.